Title
Real-time Model Parameter Estimation for Analyzing Transport in Porous Media

Authors
Juyoul Kim
Yeonjeong Park
Thomas C. Harmon

Publication Date
2003

CENTER FOR EMBEDDED NETWORKED SENSING

Technical Report Number 13

REAL-TIME MODEL PARAMETER ESTIMATION FOR ANALYZING TRANSPORT IN POROUS MEDIA

by Juyoul Kim, Yeongjeong Park and Thomas C. Harmon (tharmon@ucla.edu)

May 2003

CENS is a Science and Technology Center created by National Science Foundation under Cooperative Agreement #CCR-0120778

UCLA USC UCR CALTECH CSU JPL

Abstract. This work describes the integration of data acquisition hardware and software for the purpose acquiring not only data, but real-time transport model parameter estimates in the context of subsurface flow and transport problems. Integrated data acquisition-parameter estimation systems can be used to reduce data storage requirements, trigger event recognition and/or more detailed sampling actions, and otherwise enhance remote monitoring capabilities. The contaminant transport problem is posed here as the analogous heat transfer problem in a three-dimensional, intermediate-scale physical aquifer model. A constant source of warm water is fed into a sandy aquifer undergoing steady, unidirectional flow. The spatial distribution of temperature in the medium is monitored over time using 17 thermocouples embedded in the medium. These sensors log temperatures via conventional analog-to-digital conversion hardware driven by commercially available data acquisition software (LabVIEW™). Parameter estimation routines programmed in MATLAB™-based M-files are embedded in the LabVIEW data acquisition routine and access parameter estimation libraries, such as the descent method employed here, via the Internet. The integrated data acquisition-parameter estimation system is demonstrated for the estimation of (1) the thermal dispersion coefficients (analogous to mass dispersion coefficients), given a known heat source, and (2) the location of a heat source, given known thermal dispersion coefficients. In both cases, the parameter estimation procedure is executed repeatedly as the data are acquired. For the case of source location, the effect of the number of sensors on the parameter estimation procedure is also demonstrated. Reasonable parameter estimates are provided rapidly

during both the transient and steady state phases of the experiments, with accuracy increasing with time and with the number of observations employed.

Introduction

Ground water simulation models are used to conceptualize flow and contaminant transport enabling geoscientists to bridge data gaps in the typically under-sampled subsurface environment. While the major flow and transport processes associated with such models are understood, the specific parameters describing a given system need to be determined by calibrating ground water models according to field observations. A great deal of effort and resources are expended on subsurface sampling in support of parameter identification, and tools providing time-/cost-savings are always of the utmost interest in the field. This work describes and demonstrates the novel integration of an off-the-shelf data acquisition and model parameter identification system.

The use of real-time data analysis is common in the design and control of many engineered mechanical and chemical systems (Boaventura Cunha et al. 1997; Zupančič 1998; Perhinschi et al. 2002; Singh and Gilbreath 2002). Real-time sensing and actuation applications in biochemical process control are rapidly developing along with the state of physical (temperature, flow rate) and chemical (ionic species, dissolved oxygen, pH, etc.) sensors (Marsili-Libelli and Giovannini 1997; Bourgeois et al. 2003). The domain for these systems is typically homogeneous or of well-defined heterogeneity, and the theory describing the behavior of these systems is generally describable by arithmetic or ordinary differential equations, where conditions vary either with time or in one spatial dimension (e.g., steady state reactors). In natural environmental systems, such as ground

water, material properties are spatially distributed and often poorly defined. It is for this type of system that simulations are most helpful, and for which the development of expedited parameter estimation procedures is most challenging, and most needed.

This paper describes new procedures for integrating real-time parameter estimation routines into an automated data acquisition routine. A contaminant transport problem is posed here as the analogous heat transfer problem in a three-dimensional intermediate-scale experimental medium equipped with a conventional data-logging system for monitoring temperature in time and space. Using this system, integrated software is demonstrated for the estimation of (1) the thermal dispersion coefficients (analogous to mass dispersion coefficients), given a known heat source, and (2) the location of a constant heat source, given known thermal dispersion coefficients.

Experimental Approach and Data Acquisition System

The experiments were carried out in a physical aquifer model described previously for intermediate-scale contaminant transport experiments (Dela Barre et al. 2002). A schematic illustration of the system is shown in Figure 1. The system comprises a 150 by 50 by 35 cm deep steel and glass container. Framed stainless steel screening was used to fabricate constant head boundaries at the influent and effluent ends of the tank. Steady, unidirectional flow through the aquifer was achieved by constant peristaltic pumping into the influent clear well (Masterflex® Model 7420, Cole-Parmer, Vernon Hills, IL), while maintaining constant head conditions in the effluent clear well using a weir. The model aquifer system was packed with homogeneous, clean sand (nominal grain diameter 0.33 mm, Lonestar Sand, Monterey, CA). The sandy medium

was saturated with water to an average depth of 12 cm. The final porosity and bulk density of the model aquifer were determined to be 0.38 and 1.60 g/cm^3 (Dela Barre et al. 2002).

The experiments were carried out at pore water velocities of 0, 2.5 and 3.5 cm/h. For each experiment, a continuous 31.6 mL/min source of warm water was introduced at a fixed location via the same peristaltic pump equipped with small precision tube (1.6 mm i.d., Masterflex® L/S™ 14). Seventeen thermocouples (J type, 1.5 mm o.d.) were installed as indicated in Figure 1 to monitor three-dimensional temperature distributions resulting from point source injection. One of these thermocouples was fixed to the outlet of the warm water injection tube to monitor the source temperature.

The automated monitoring system (Figure 1) was fabricated using off-the-shelf equipment. The thermocouple network was connected to signal conditioning and analog-to-digital switching modules (National Instruments (NI), SCXI-1303, -1326) mounted on a 12-slot chassis (NI SCXI-1001). This chassis serves to power the SCXI modules while handling timing, trigger, and signal routing between the digitizer and SCXI modules. The chassis was connected to 16-bit data acquisition (DAQ) card (NI DAQCard™-AI-16XE-50), which was connected to a PC via a PCMCIA card. The DAQ system was controlled using LabVIEW (v6.1, NI) software, which employs an object-oriented programming language called Virtual Instrument (VI) to create graphical users interface (GUI) for creating input and displaying output (Figure 2). MATLAB (v6.5, The MathWorks, Inc.) routines were embedded into the LabVIEW program using the MATLAB ActiveX automation server to support the mathematical modeling and parameter estimation approaches discussed below.

Heat Transport Theory

The analogy between heat and mass transfer is exploited to take advantage of the small form factor and low cost of temperature sensors relative to those for dissolved mass. As chemical sensors develop, the approaches described here can be applied to mass transport problems. The heat-mass transfer analogy is valid if the following conditions apply (Eckert and Drake 1987; Bird et al. 2002): physical properties are constant in time, no heat or mass is produced in the system (e.g., no chemical reaction), no radiant energy is emitted or absorbed, no viscous energy is dissipated, and the velocity is not affected by heat or mass transfer.

Here we consider the problem of a continuous point heat source in a three-dimensional, homogeneous porous medium under steady, uniform flow conditions. The governing equations for the transient heat transport are:

$$\frac{\partial T(t,x,y,z)}{\partial t} = \kappa_x \frac{\partial^2 T}{\partial x^2} + \kappa_y \frac{\partial^2 T}{\partial y^2} + \kappa_z \frac{\partial^2 T}{\partial z^2} - u_x \frac{\partial T}{\partial x} + Q(t,x,y,z) \qquad (1)$$

I.C. $T(0,x,y,z) = T_0$ (2)

B.C. $T(t,\pm\infty,y,z) = T_0$, $T(t,x,\pm\infty,z) = T_0$, $T(t,x,y,\pm\infty) = T_0$ (3)

where $Q(t,x,y,z) = q(t)\delta(x-x_0)\delta(y-y_0)\delta(z-z_0)$ (4)

where T is temperature, u_x is the pore water velocity, κ_x, κ_y and κ_z (cm^2/min) are the longitudinal and transverse thermal dispersion coefficients (analogous to hydrodynamic dispersion coefficients in the well-known mass transport equation), T_0 is the initial uniform temperature in the medium, q and Q are the volumetric and overall rates of heat input at a single point in space. Thermal dispersion coefficients contain

components for pure diffusion and dispersion due to advection: $\kappa_i = \kappa_e + \beta_i \cdot u_x$ for each direction $i = x, y, z$ (analogous to hydrodynamic dispersion coefficients), where κ_e is the thermal diffusion coefficient (cm^2/min), and β_i is thermal dispersivity (cm).

If the heat is liberated at a rate $q(t)$ from $t = 0$ to $t = t_f$ at the point (x_0, y_0, z_0), an analytical solution for the continuous point heat source is then (Carslaw and Jaeger 1986):

$$T(t,x,y,z) = T_0 + \frac{1}{8(\pi^3 \kappa_x \kappa_y \kappa_z)^{1/2}} \int_0^{t_f} \frac{q(t)}{t^{3/2}} \cdot \exp\left\{ -\frac{1}{4t} \left[\frac{(x - x_0 - u_x t)^2}{\kappa_x} + \frac{(y - y_0)^2}{\kappa_y} + \frac{(z - z_0)^2}{\kappa_z} \right] \right\} dt \quad (5)$$

If the source is constant ($q(t) = q_0$), then q_0 is defined by experimental conditions as the product of the source temperature (ºC) and injection rate (mL/min).

Parameter Estimation Algorithm

For the above heat transport model, we formulated algorithms to use observed temperature distributions to identify (1) optimal thermal dispersion coefficients, given the source conditions, or (2) the best-estimate of the source location, given the thermal dispersion coefficients. Both cases can be described as inverse problems which can be solved by minimizing sum of the squared errors between the calculated and observed temperature values. Temperature observations are available only at discrete locations and times, so the problem expressed in terms of the objective function $\mathbf{\Phi}$ is:

$$\min \mathbf{\Phi}(\mathbf{p}) = \sum_{m=1}^{M} w_m^2 \left(T_m(\mathbf{p}) - T_m^{obs} \right)^2 \quad (6)$$

where $T_m(\mathbf{p})$ is the calculated temperature, T_m^{obs} is the observed temperature, M is the number of observations in space, w_m is a weight associated to measurement m, and $\mathbf{p} = (\kappa_x, \kappa_y, \kappa_z)$, the vector of thermal dispersion coefficients, or $\mathbf{p} = (x_0, y_0, z_0)$, the source location, to be identified. Here, the minimization problem is solved using the Levenberg-Marquardt (L-M) method, which is a descent method that has been used to identify source terms in contaminant transport models (Levenberg 1944; Marquardt 1963; Sun 1995; Sciortino et al. 2000).

The L-M method determines sequential parameter vector estimates as follows.

$$\mathbf{p}_{n+1} = \mathbf{p}_n - \left(\mathbf{A}_n^T \mathbf{W} \mathbf{A}_n + \lambda \mathbf{I} \right)^{-1} \mathbf{A}_n^T \mathbf{W} \mathbf{f}_n \tag{7}$$

where n is the iteration number, the term inside the parentheses is an approximation of the Hessian matrix, $\mathbf{A}_n$ is the matrix of partial derivatives (the Jacobian matrix) of the temperature function, and $\mathbf{f}_n$ is the vector of residual values for the current iteration:

$$\mathbf{f}_n = \begin{bmatrix} T_1(\mathbf{p}) - T_1^{obs} \\ \vdots \\ T_M(\mathbf{p}) - T_M^{obs} \end{bmatrix} \tag{8}$$

In (7), $\lambda \mathbf{I}$ is a correction term, where λ is an adjustable constant and $\mathbf{I}$ is the identity matrix. $\mathbf{W}$ is a diagonal matrix whose elements represent the weights w_m associated with each element of the residual vector $\mathbf{f}_n$. The purpose of this term is to guarantee that the estimated objective function decreases from one iteration to the next, and that the parameter vector is within the range of admissible values.

A flow chart summary of the L-M algorithm in the context of current DAQ system is provided in Figure 2. The L-M requires an initial parameter vector estimate, which is supplied by the user in the LabVIEW environment. The user also must specify the frequency with which the L-M algorithm collects current temperature measurements from the sensors and estimates the parameters. Then, temperatures and their derivatives with respect to the parameter vector are determined analytically from (5), and the Jacobian matrix for the temperature function is calculated, and used to estimate the Hessian matrix:

$$\mathbf{H}_n \cong \mathbf{A}_n^T \mathbf{W} \mathbf{A}_n + \lambda \mathbf{I} \tag{9}$$

The Hessian matrix (9) is then used in equation (7) to determine the next parameter estimate. The process repeats until either the gradient of the objective function or the change from the previous value of the objective function is below a user-prescribed tolerance (1×10^{-4}). The solution of Eq. (6) converged prior to 100 iterations in most cases, with the overall computational time increasing with the density of data collection (M) from several seconds to several minutes.

The L-M parameter optimization algorithm was embedded in the DAQ system and employed to estimate either thermal dispersion coefficients or the source location. The real-time parameter estimating process was first exercised by estimating and updating either of these parameters (knowing the correct values of the others) throughout the transient portion of the experiments until quasi-steady-state conditions were achieved. In a second experiment, the source location was estimated using the L-M routine, varying the number of observations employed.

Results and Discussion

Three-dimensional temperature distributions were collected over time for three velocities using the thermocouple configuration shown in Figure 1. Typical temperature histories collected a probes located at the source, and along the downstream centerline (y = 20 cm), are plotted in Figure 3 for a velocity of 2.5 cm/h. The average temperature measured at the source location (observation channel 7) was 57.3 ± 1.0 $^{\circ}$C. The source temperature was nearly constant, except for during the initial injection period. During this start-up period, heat exchange between the warm source water and the tubing (initially at the ambient temperature) was unavoidable. After approximately 120 minutes, most of the sampling network had achieved steady-state. Exceptions were points furthest from the source (e.g., channel 17), which failed to achieve steady-state conditions over the time scale of the experiment as evidenced by the ongoing, albeit modest, temperature increases exhibited there at the end of the experiment. In general, the parameter estimation procedure is expected to be more feasible for a steady-state data case because knowledge of the source history is not necessary, and the inverse problem is less sensitive to occasional sampling errors (Sciortino et al., 2000).

The plot in Figure 4 compares observed and optimized steady-state temperature distributions in the x-y plane (z = 6 cm). This comparison indicates generally good agreement between the measured temperature distributions and analytical heat transport solutions, with local discrepancies more pronounced near the source. These discrepancies are an artifact of the source injection method in the experimental system, which caused the development of local flow field anomalies in the otherwise unidirectional flow field. The local complexities stemming from this flow perturbation are not captured by the relatively simple model employed.

The plot in Figure 5 tracks the history of thermal dispersion coefficients estimated in real-time at a single point (observation channel 14: x = 30, y = 20, z = 6 cm) at two flow velocities. For these cases, the parameter estimation routine was initiated 15 minutes after the initiation of the experiment to avoid the start-up time anomalies noted previously with respect to the source. Three parameters (i.e., longitudinal, lateral, and vertical coefficients) were estimated and updated using temperatures acquired every five minutes. The first parameter estimates for the 2.5 cm/h velocity are inconsistent and were probably affected by the source start-up period. This problem is alleviated by the second data acquisition event. From the second sampling event on, there is an increase in the parameter estimates followed by an asymptotic approach to their steady-state values. All of the parameter estimates were reasonable when compared with the given thermal dispersion coefficient of sand-water medium for zero velocity (0.34 cm^2/min). For the lower velocity, the final estimates (0.51, 0.52, and 0.52 cm^2/min for a longitudinal, lateral, and vertical direction, respectively) were the same regardless of orientation relative to flow. At 3.5 cm/hr, the longitudinal thermal dispersion coefficient (0.73 cm^2/min) became distinguishable from transverse values (both roughly 0.44 cm^2/min), as shown in Figure 5(b).

The indistinguishable longitudinal and transverse parameter estimates at the lower velocity may have been another artifact of the local flow anomaly created by the source flow (discussed above). As the system velocity decreases, the local source flow becomes more significant. This explanation points to the sensitivity of this real-time estimation algorithm to artifacts introduced by experimental conditions. To compare observations to

theory in real time, in effect to question a conceptual model for a system, would be highly desirable capability in support of many types of hydrogeologic investigations.

The plots in Figure 6 demonstrate (1) the quality of fits for parameters identified 120 minutes into the experiment and (2) the inclusion of parameter uncertainty principles to the optimization procedure. The results in Figure 6a are for the optimized thermal dispersion coefficients, given the source location. Those in Figure 6b are based on optimizing the source location, given knowledge of the thermal dispersion coefficients. In all cases, the simulated behavior from the best parameter estimates is encompassed by simulations based on the 95% confidence intervals for those parameters. Including the confidence interval allows one to gauge the quality of model-observation agreement more objectively. Here, for sampling locations closer to the source, observations were collected outside of the confidence interval. This result could be used as an indication that (1) the theory being applied inadequately captures the relevant system dynamics, (2) there are experimental artifacts to be accounted for, or (3) some combination of both of these issues.

In the final test of the real-time parameter estimation program, temperature data were acquired until a quasi-steady-state distribution was achieved (120 minutes). Given the previously estimated thermal dispersion coefficient values, the source location was estimated at several times (35, 60, 90 and 120 min). At each of these times, the number of observation points (m) was also varied from 1 to 16. In all cases, the algorithm used the origin of the experimental coordinate system as an initial estimate of the source location. The embedded algorithm does not address the problem of optimal combinations of observations, which is a computationally demanding problem addressed elsewhere

(Sciortino et al., 2002). Instead, the sensors employed were selected in order of the channel numbers system shown in Figure 1 (e.g., 1 sensor = Ch 1, 2 sensors = Chs. 1 and 2, etc.).

The points in Figures 7a-b depict the final (120 min) sequence of source locations predicted for designated number of observations in the horizontal (x-y) and vertical (x-z) planes, respectively. As expected, the accuracy of the source estimate increases significantly over the transition from a sparsely to densely sampled system. For the present problem, the increases in accuracy begin to diminish beyond about 9 or 10 observation points. The accuracy for the source location problem here is greater in the x-y plane than it is vertically (Fig. 7a *vs* 7b), suggesting that the problem was under-sampled in the vertical dimension. There is clearly a tradeoff between accuracy and computation efficiency in these types of problems. For a small number of observations, the source location computations required only seconds to complete, but are less accurate. As the number of observations increases, so does accuracy, but the computations require minutes to complete. The minimum temporal scale or interval required for such calculations is problem-dependent. For many problems involving groundwater flow and transport, executing more computationally intensive calculations on an infrequent basis would be sufficient. Other problems, such as well hydraulic tests, or small scale tracer tests, may require more frequent execution of a parameter estimation routine. As sensor network technology matures, the spatial sampling density problem will become the more relevant one in the field of hydrogeology. Thus, additional research is warranted to develop monitoring network design strategies aimed at optimal sensor density in heterogeneous subsurface domains.

Summary and Conclusions

This work describes the development and testing of a real-time heat transport parameter and source identification algorithm that was developed by embedding a MATLAB-based parameter optimization routine into a LabVIEW-based DAQ system. The integrated software was shown to provide reasonable of heat transfer parameters (thermal dispersion coefficients) for a test case involving a constant point source in a saturated porous medium subject to unidirectional flow. The results suggested that this approach was sufficiently robust to withstand early transient effects and arrive at reliable parameter estimates as early as temporal observational density allows. Discrepancies between model simulations and observations can be scrutinized in real-time through the inclusion of parameter estimate confidence intervals in the analysis.

This main purpose of this work is to demonstrate the potential for engineers and earth scientists to connect environmental sensors with information technologies more advanced than simple data-logging devices. In contaminant hydrogeology, real-time parameter estimation procedures could be made immediately available for pump tests or other commonly applied field tests. On projects with longer time scales (e.g., demonstrating monitored natural attenuation), such techniques could be used to automated long-term, intermittent sampling and documentation of oxidation-reduction conditions. As sensor network modalities expand to encompass more environmental species, potential applications for real-time parameter estimation and monitoring network design tools will expand rapidly.

Acknowledgements. Funding from the UCLA's Center for Embedded Networked Sensing (CENS) under cooperative agreement #CCR-0120778 with the National Science Foundation is gratefully acknowledged. The ideas, equipment and software used in this research have not undergone agency review, and their descriptions and usage do not imply agency endorsement.

References

Bird, R.B., W.E. Stewart, and E.N. Lightfoot. 2002. *Transport phenomena* 2nd ed., J. Wiley, New York.

Boaventura Cunha, J., C. Couto, and A.E. Ruano. 1997. Real-time parameter estimation of dynamic temperature models for greenhouse environmental control. *Control Engineering Practice* 5, no. 10: 1473-1481.

Bourgeois, W., P. Hogben, A. Pike, and R.M. Stuetz. 2003. Development of a sensor array based measurement system for continuous monitoring of water and wastewater. *Sensors and Actuators B* 88: 312-319.

Carslaw, H.S. and J.C. Jaeger. 1986. Conduction of heat in solids 2nd ed., Oxford University Press.

Dela Barre, B.K., T.C. Harmon, and C.V. Chrysikopoulos. 2002. Measuring and modeling the dissolution of nonideally shaped dense nonaqueous phase liquid pools in saturated porous media. *Water Resources Research* 38, no. 8: U143-U156.

Eckert, E.R.G. and R.M. Drake, Jr. 1987. *Analysis of heat and mass transfer*. Hemisphere Publishing Corporation.

LabVIEW v6.1. 2001. National Instruments. Available from http://www.ni.com/

Levenberg, K. 1944. A method for the solution of certain problems in least squares. *Quarterly AppIied Math* 2: 164-168.

Marquardt, D. 1963. An algorithm for least-squares estimation of nonlinear parameters. *SIAM Journal Applied Math* 11: 431-441.

Marsili-Libelli, S. and F. Giovannini. 1997. On-line estimation of the nitrification process. *Water Research* 31, no. 1: 179-185.

MATLAB v6.5. 2002. The MathWorks, Inc. Available from http://www.mathworks.com/

Perhinschi, M.G., G. Campa, M.R. Napolitano, M. Lando, L. Massotti, and M.L. Fravolini. 2002. A simulation tool for on-line real time parameter identification. *American Institute of Aeronautics and Astronautics Modeling and Simulation Technologies Conference and Exhibit*, Monterey, CA.

Sciortino, A., T.C. Harmon, and W.W-G. Yeh. 2000. Inverse modeling for locating dense nonaqueous pools in groundwater under steady flow conditions. *Water Resources Research* 36, no. 7: 1723-1735.

Sciortino, A., T.C. Harmon and W. W-G. Yeh. 2002. Experimental Design and Model Parameter Estimation for Locating a Dissolving DNAPL Pool in Groundwater, *Water Resources Research*, 38, no. 5: U290-U298.

Singh, R. and G. Gilbreath. 2002. A real-time information system for multivariate statistical process control. *International Journal of Production Economics* 75: 161-172.

Sun, N-Z. 1995. *Inverse problems in groundwater modeling*. Kluwer Academic Publishers, the Netherland.

Zupančič, B. 1998. Extension software for real-time control system design and implementation with MATLAB-SIMULINK. *Simulation Practice and Theory* 6: 703-719.

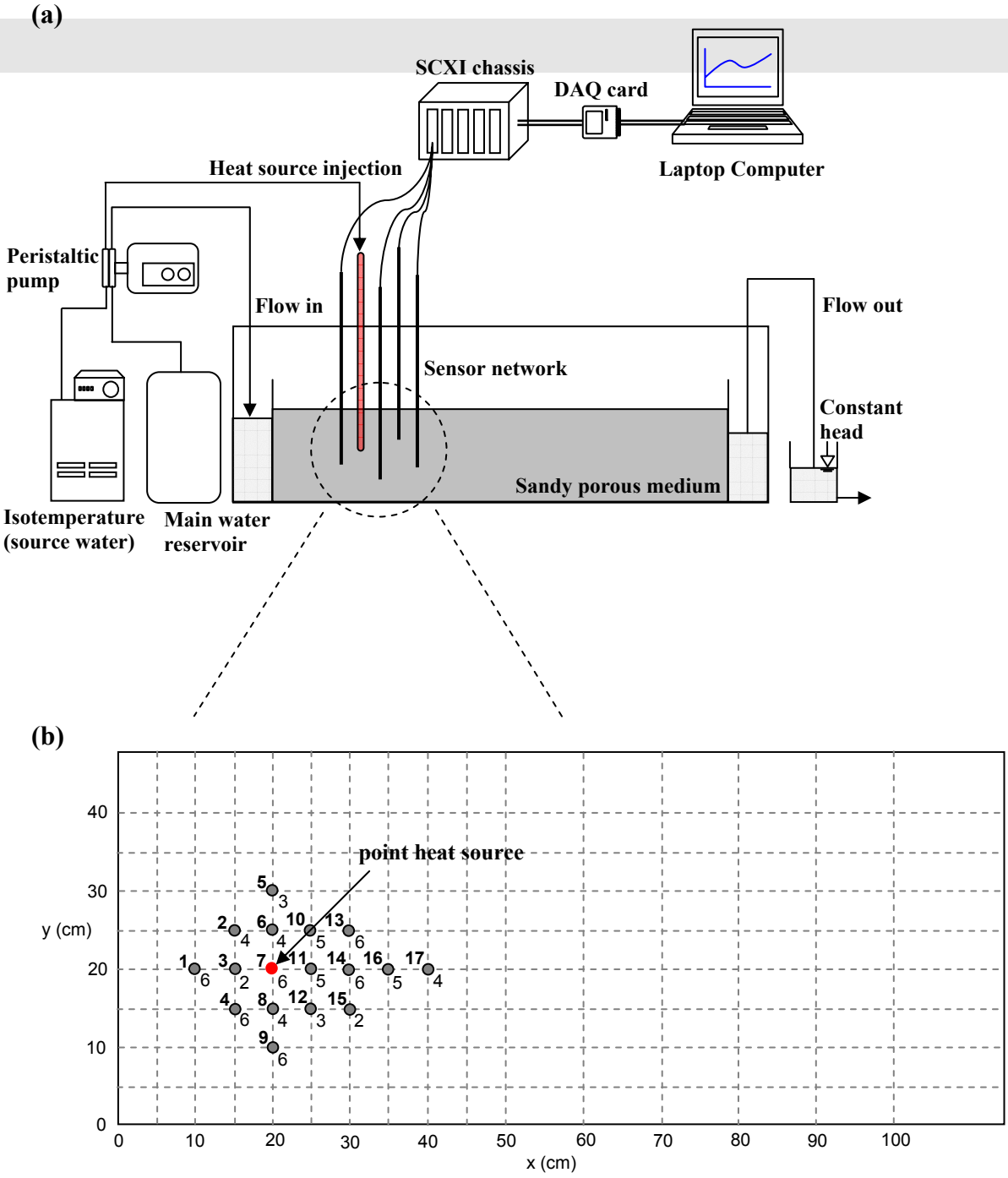

Figure 1. Schematic diagram of (a) the experimental and data acquisition systems and (b) plan view of test box showing the thermocouple deployment: symbols represent source input and sampling locations (bold number to the upper left of each symbol indicates the sampling channel number; number to the lower right indicates the elevation (cm) of the thermocouple relative to the bottom of the test box).

(a)

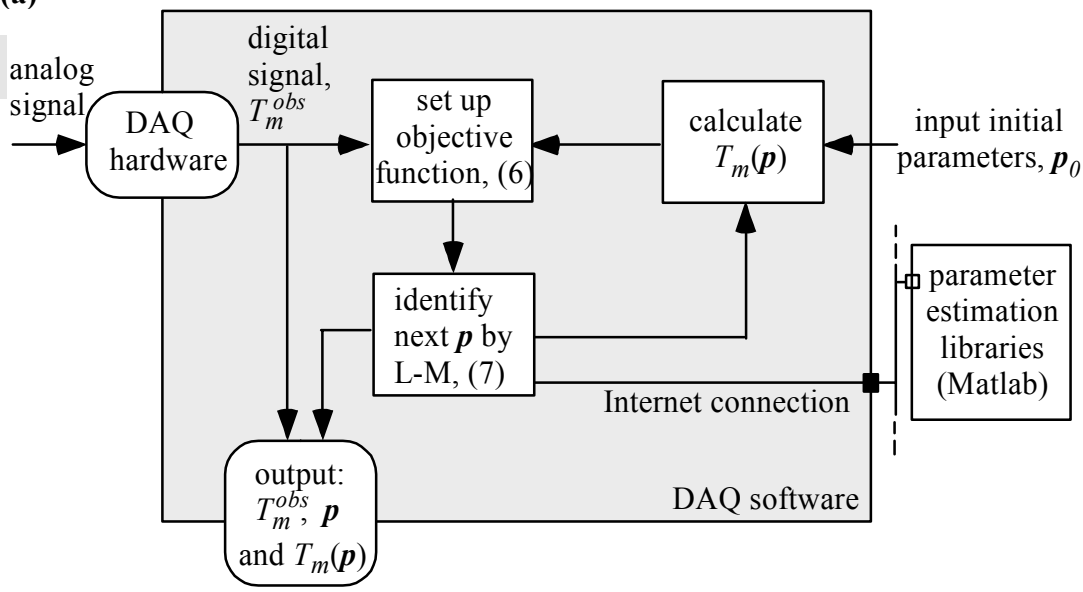

(b)

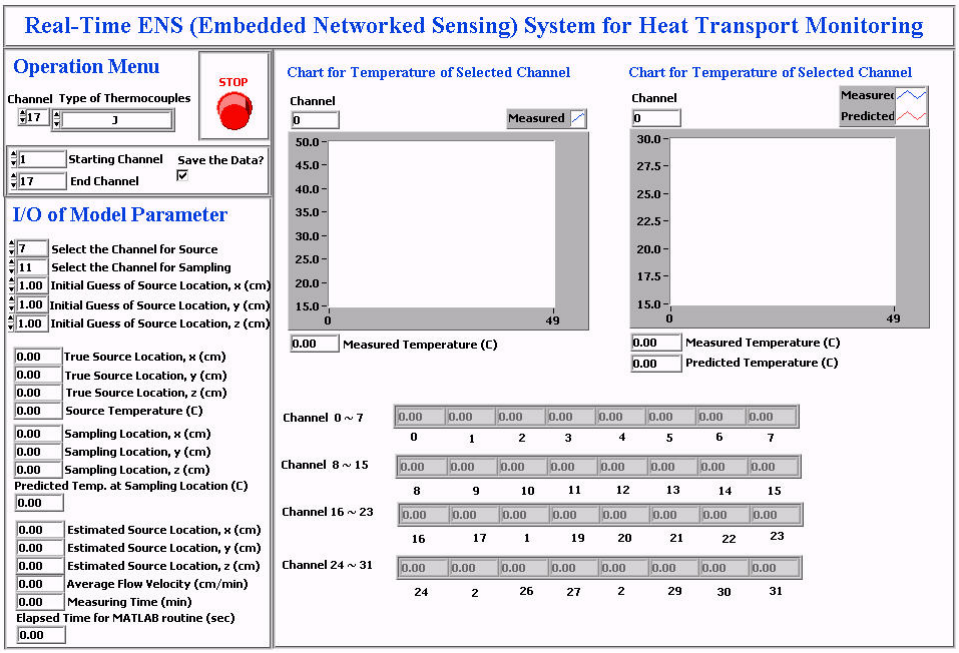

Figure 2. (a) Flowchart of data acquisition and parameter estimation software functions and (b) a screen-capture of the LabVIEW GUI for the data acquisition and source location estimation routine.

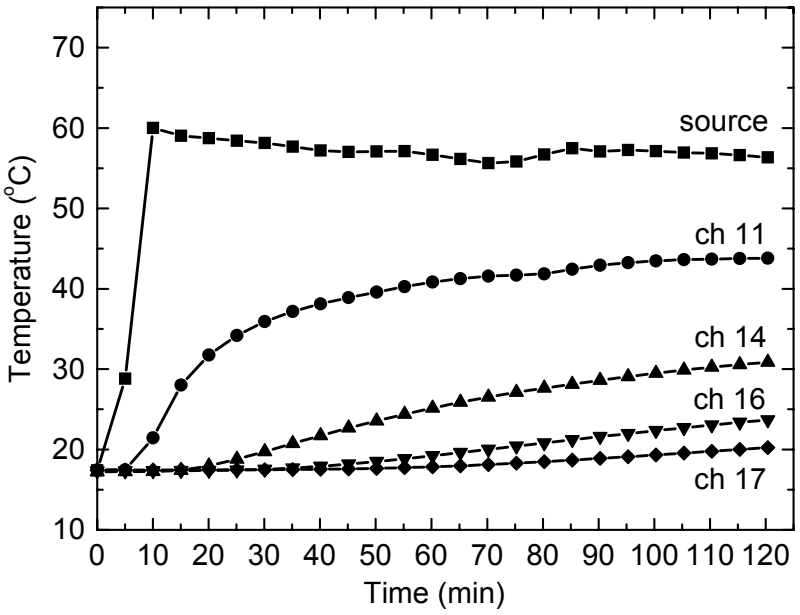

Figure 3. Observed temperature profiles along the centerline of test box downstream of the source for flow velocity of 2.5 cm/hr (ch = channel or sampling location).

(a)

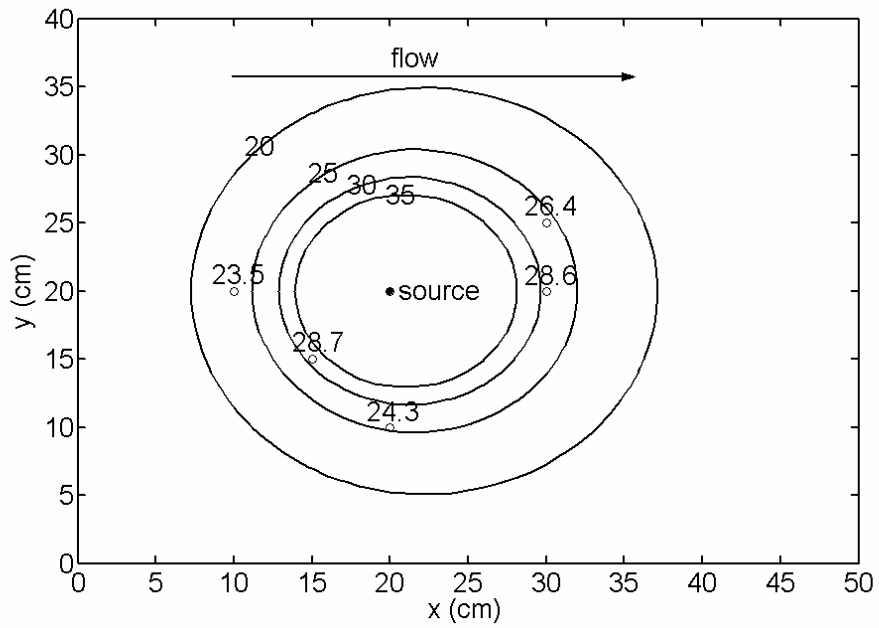

(b)

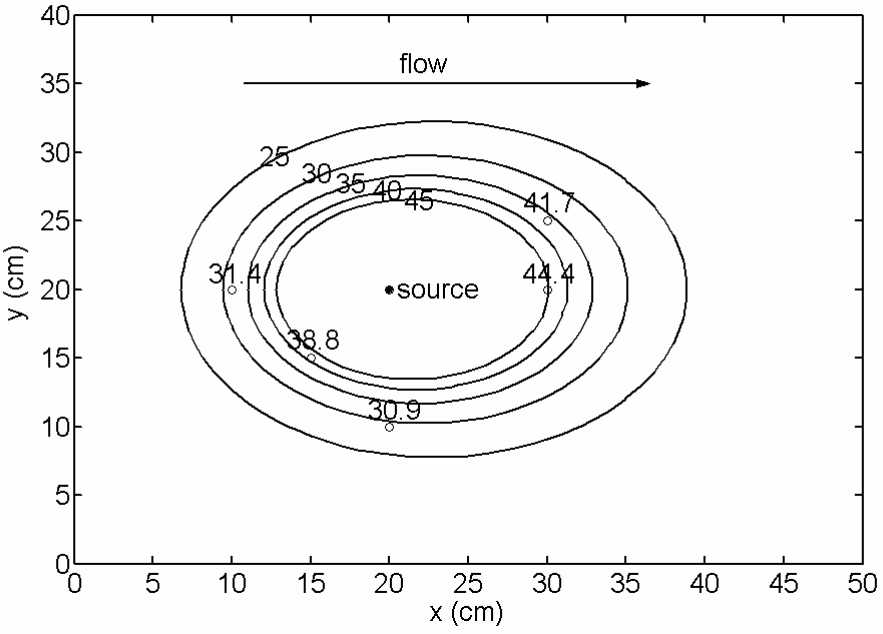

Figure 4. A comparison of simulated (contoured) and observed (symbols) temperature (^{o}C) in the x-y plane at elevation z = 6 cm for (a) velocity = 2.5 cm/hr at 120 min and (b) velocity = 3.5 cm/h at 90 min.

(a)

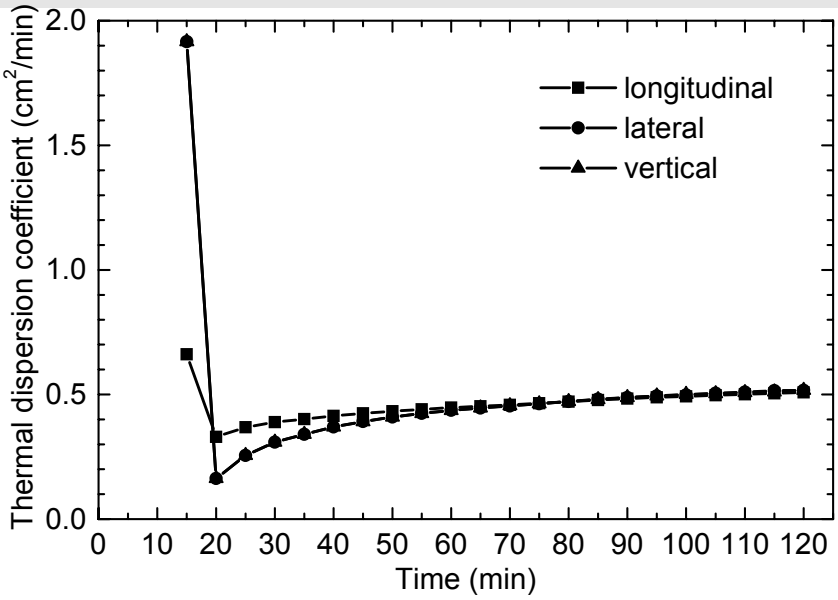

(b)

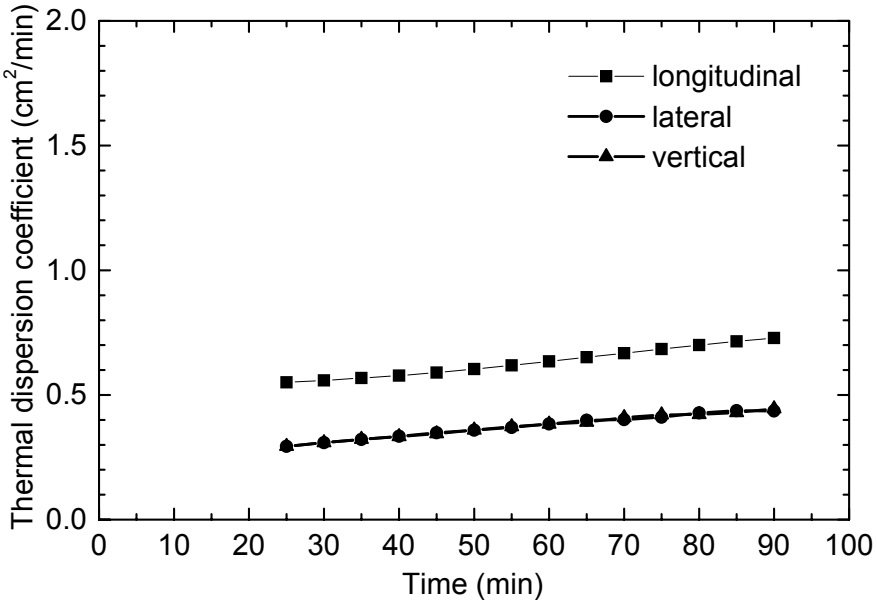

Figure 5. The sequence of estimated thermal dispersion coefficients for flow velocities of (a) 2.5 and (b) 3.5 cm/hr at a distance of 10 cm directly downstream of the source (ch 14).

(a)

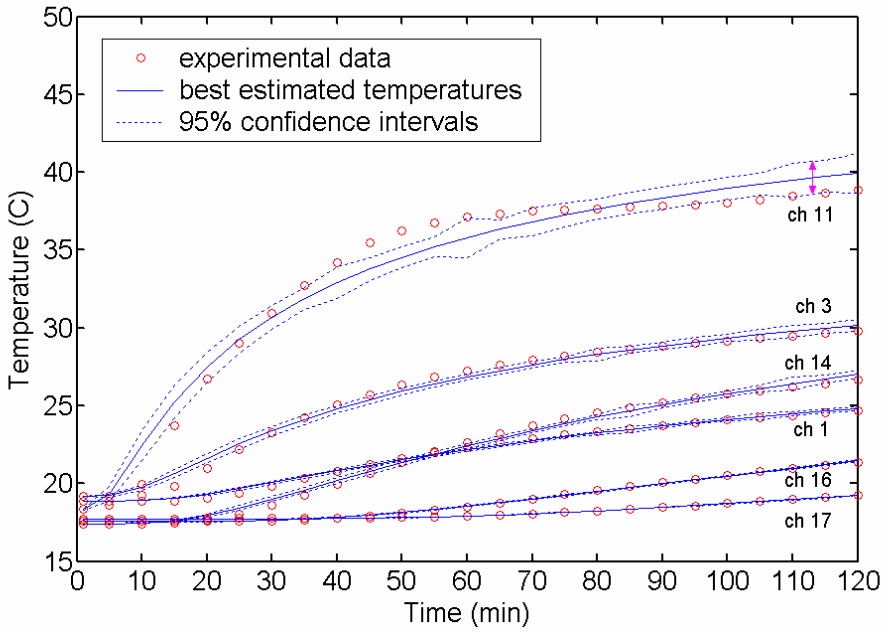

(b)

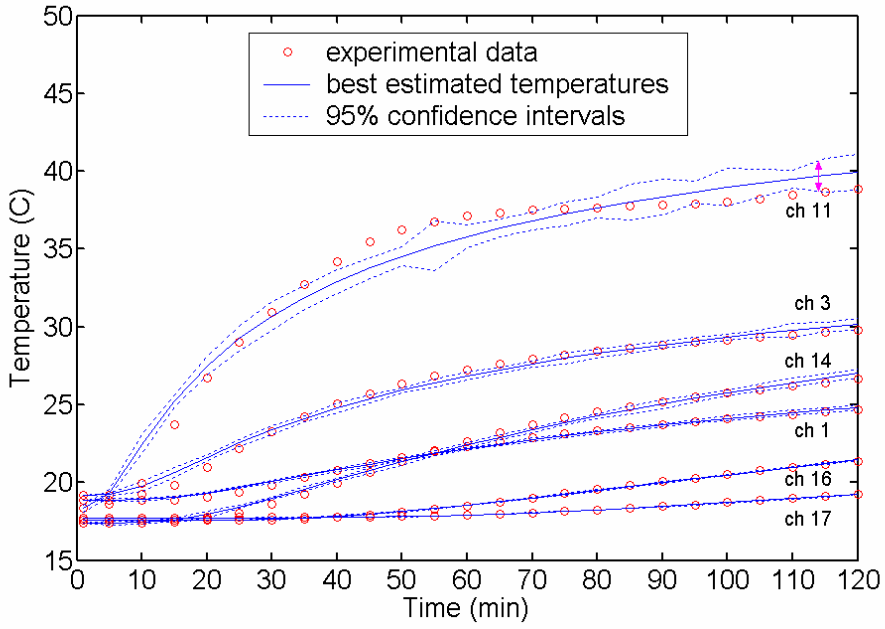

Figure 6. Comparison of experimental observations (symbols) and model simulations optimized with respect to (a) thermal dispersion coefficients and (b) source location (dashed lines designate simulations based on the estimated parameters' 95% confidence intervals).

(a)

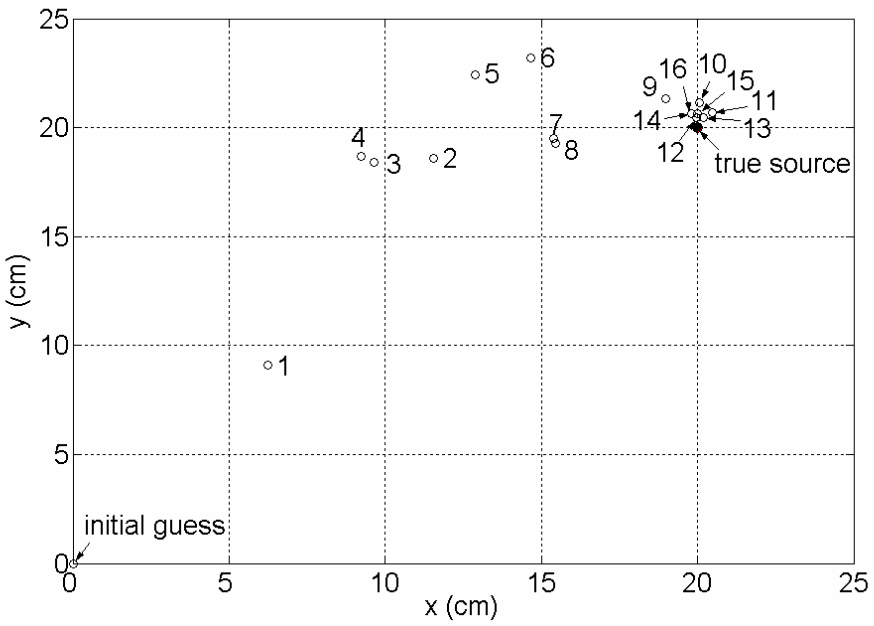

(b)

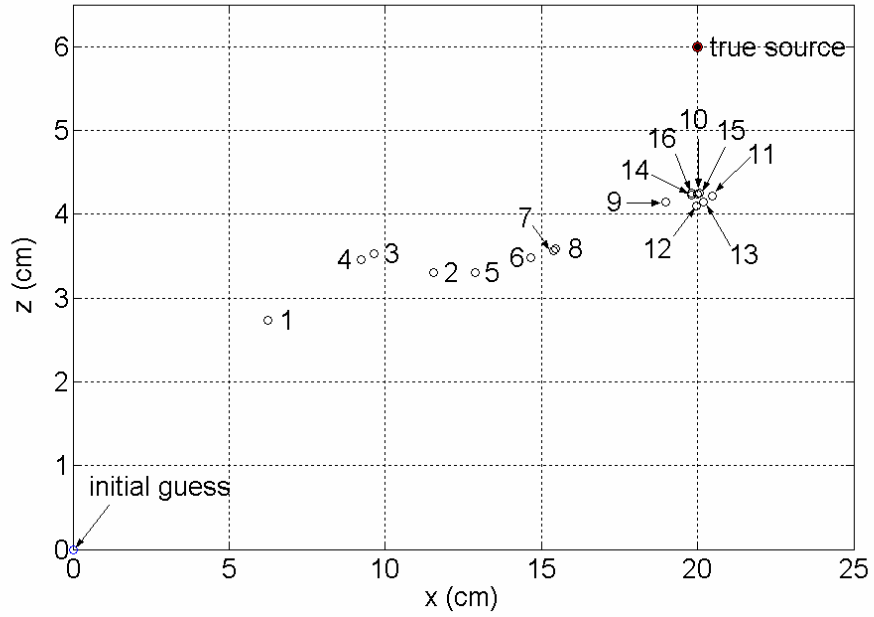

Figure 7. The progression of source location estimates (symbols) in the (a) x-y and (b) x-z planes based on successively increasing numbers of sensors (sensors used were taken sequentially be channel number as described in text; initial location estimate was in all cases the origin (origin) and true source location was (20, 20, 6); thermal dispersion coefficients were known; velocity = 0 cm/h).